

THE EFFECTS OF AIR ENTRAINMENT ON VACUUM DRIVE ROLLER TRACTION

by

J. N. Dobbs
3M
USA

ABSTRACT

Vacuum assisted drive rollers are commonly used to provide additional traction in web tension control schemes. Single-sided web contact makes them a natural choice between a coating station and an oven where lower tensions are often desired. Many vacuum rollers are designed by the manufacturer according to customer provided specifications, and very little is published on their effective traction capacity where air entrainment is significant. In this paper, an empirical study is carried out to measure the traction on a vacuum drive roller as a function of vacuum level, web tension and speed. Loss of traction is determined by measuring the differential velocity between the web and vacuum roller surface in conjunction with the inability to maintain a programmed tension differential across the roller. Comparison is made between experimental measurements and the traction that would be expected for a simply wrapped roller.

NOMENCLATURE

β	Web wrap around vacuum pull roller (radians)
μ	Coefficient of friction (including air lubrication effects)
μ_0	Initial slowly sliding coefficient of friction
μ_f	High speed residual coefficient of friction
η	Viscosity of air (Pa s)
n	Number of grooves under the web
h_0	Entrained air layer float height (μm)
R	Roller radius (m)
R_q	Roller surface roughness (μm)
S_g	Cross sectional area of a groove (mm^2)
T_{in}	Web tension entering vacuum pull roller (N)
T_{out}	Web tension exiting vacuum pull roller (N)
T_{pli}	Web tension per unit web width (N/m)
V	Web velocity (m/s)

INTRODUCTION

Vacuum assisted drive rollers can be used to provide large changes in web tension and are a good alternative to nipped drive rollers where two sided web contact is not permitted. Simply wrapped drive rollers can rarely achieve more than a two to one change in web tension and provide no tension at all if the web is slack. Vacuum drive rollers suffer neither of these limitations and are often used between a coating station and an oven where relatively high tension is desired for coating and low tension is necessary to prevent web damage in a hot oven. Vacuum drive rollers are expensive ranging from \$25,000 for a laboratory sized roller to \$150,000 for a 2m wide roller. These costs do not include the motor drive or the vacuum blower and piping required for the roller. Much of the expense of a vacuum roller is in drilling the vacuum holes and machining the surface of the roller. Vacuum roller diameters, as provided by the manufacturer, tend to scale rapidly with width often reaching 0.5m in diameter for a 2m wide roller. This rapid increase in roller surface area contributes to the high cost of the roller.

Two basic vacuum roller designs are commonly used with variations. The first design consists of a roller shell with vacuum holes or slots machined through where the outside of the shell forms the surface of the roller. Occasionally, the shell may have an elastomeric cover but nevertheless, the vacuum holes are drilled straight through and are typically spaced 25 to 50 mm apart from each other on the roller surface. Another variation on this basic design is to machine vacuum distribution grooves on the roller surface which intersect the holes. The second basic vacuum roller design consists of an inner structural shell with through holes or slots, covered by a porous screen or thin perforated shell which provides vacuum distribution on a scale of 2 to 4 mm. One advantage of the first design is the relative ease of cleaning fewer and larger holes and grooves. The second design presents many but smaller holes to the web, which may prevent embossing of delicate web materials.

One purpose of this study was to provide empirical measurements of vacuum drive roller traction as a function of web speed. As web lines are operated at faster line speeds, it is important for these rollers to be designed and operated so as to prevent slippage and damage to the web. Another purpose of the study was to try and determine what some of the mechanisms were that contributed to vacuum roller traction. These factors could then be used to select an appropriate roller design for a particular web line application.

ROLLER TRACTION THEORY

Many theories have been developed to predict web traction over idler rollers, some of these including the effects of air entrainment as well as the grooving or surface patterning of rollers used to combat this problem. The belt equation

$$T_{out} = T_{in} e^{\mu \cdot \beta} \quad (1)$$

is often used to determine the maximum output tension, T_{out} , that can be obtained for a given input tension, T_{in} , coefficient of friction, μ , and wrap angle, β , of the web around the roller. Friction is reduced by air entrainment using the foil bearing equation (Ref. 1)

$$h_o = 0.65R \left[\frac{12 \cdot \eta \cdot V}{T_{pli}} \right]^{\frac{2}{3}} \quad (2)$$

where the web float height, h_0 , is given as a function of the roller radius, R , air viscosity, η , web velocity, V , and tension per unit web width, T_{pli} . Equation (2) was developed for rollers with random surface topology but has also been applied grooved rollers using the following modification by Hashimoto (Ref. 2)

$$h = h_0 - \frac{n \cdot s_g}{W} \quad (3)$$

where n is the number of grooves under the web of width W and s_g is the sectional area of a groove. Equation (3) was conceived for a roller with circumferential grooves and does not take into account the holes drilled through the shell. Hashimoto also calculated numerical solutions for pressurized porous roller shells, which may have application in the case with no vacuum if there is any internal pumping¹ of air at high speeds. Complex roller surfaces with grooves or patterning most likely require computational solutions (Refs. 3, 4), but reasonable results have been obtained with the following expression (Ref. 5).

$$\begin{aligned} \mu &= \mu_0 & h &\leq R_q \\ \mu &= \mu_0 - \left(\frac{\mu_0 - \mu_f}{2} \right) \cdot \left(\frac{h}{R_q} - 1 \right) & R_q &\leq h \leq 3R_q \\ \mu &= \mu_f & h &\geq 3R_q \end{aligned} \quad (4)$$

That is, the air lubricated coefficient of friction, μ , is equal to the initial slowly sliding coefficient of friction, μ_0 , until an air layer, h , has developed equal to the roller surface roughness, R_q . The friction then decreases linearly with increasing air layer height until it reaches a final residual friction, μ_f , when h is equal to three times R_q . Traction computations using equations (1) through (4) would best apply where there is low input tension, and therefore larger air layer, with no applied vacuum.

EXPERIMENTAL TEST METHOD

The vacuum drive roller used in this study was of the first design type with drilled through holes and grooves machined into its surface. Figure 1 shows the hole and groove pattern used along with the machine direction (MD) and cross machine direction (CMD) hole spacing used. Grooves were square in section with a width of 1.25 mm and depth of 0.25 mm. Holes and grooves together covered 14.5% of the total surface area of the eight inch diameter roller. Internal seals and externally applied masking tape were used to limit the vacuum to the area covered by the web. Static vacuum levels, measured in the center of the roller, in excess of 13kPa were achieved and, given the very small flows observed, should be representative of the vacuum delivered to the roller surface. Measurement of the chrome plated roller surface indicated a surface roughness $R_a = 0.45$ microns between the vacuum grooves.

Polyethylene terephthalate (PET) web 30.5 cm in width and 25 microns in thickness was used for all traction testing. This material is commonly used for tape substrates and removable liners and is smooth enough to present a significant traction challenge for

¹ This may not be as strange as it seems since the bottom side of the vacuum roller is open to atmosphere and an internal boundary layer of air will be carried into the vacuum seals and possibly forced through the shell under the web.

many roller surfaces. Slowly sliding coefficient of friction, μ_0 , between a web sample and the roller was measured to be 0.4. Web line geometry near the test roller is shown in Figure 2 with a web wrap, β , around the vacuum roller of 2.75 radians.

For this study, the vacuum drive roller was used as the pacing roller for the web line. This ensured a known and constant speed for this roller, measured (Ref. 6) nearby as indicated in Figure 2 using a laser doppler velocimeter (LDV). At the beginning of each traction test, a tension, T_{in} , was established for the web entering the vacuum roller. The outgoing tension, T_{out} , was initially set to equal T_{in} and then slowly ramped up to the maximum web line tension capability of 315 N or ramped down to the minimum tension capability of 1 N. As this tension differential reached the traction capacity of the vacuum roller, the speed measured by the LDV would deviate from the line pacing speed, indicating slippage on the roller. Figure 3 shows T_{in} , T_{out} and web speed plotted as a function of time for one of the test runs. This figure is representative of traction runs made at slower speeds where loss of traction on the vacuum roller would result in a stick-slip operation of the web line as it attempted to maintain the programmed tension ramp. For high speed tests, the web speed would increase in a smooth fashion until it reached the maximum or minimum speed limit of the next driven roller. Loss of traction could also be detected audibly as a high pitched hum.

VACUUM TRACTION MEASUREMENTS

A series of traction experiments were made for web speeds from 6 to 305 m/min, vacuum levels from 0 to 12.5 kPa and input web tensions from 25 to 215 N (0.5 pli to 4 pli). Data for these experiments are summarized in Table 1 for $T_{out} > T_{in}$ and Table 2 for $T_{out} < T_{in}$. Values for the input and output web tensions, T_{in} and T_{out} , shown in the table were established for the onset of slippage on the vacuum roller by examining data plots such as Figure 3 for each experimental test condition. For quite a number of test conditions, no web slippage could be developed across the vacuum roller due to the 315 N upper and 1 N lower tension limits for the web line. These points are indicated by an asterisk (*) in the table and were not used for any subsequent data analysis or graphs. In fact, it was remarkably difficult to get web slippage for the tension conditions in Table 2.

One useful method for assessing the effectiveness of a driven roller is to look at the ratio of high to low tension that can be achieved before the web slips on the roller. Use of these ratios permits a comparison between many different input tension values that a tension difference measure cannot. Obviously, a tension ratio of one indicates a roller that is unable to apply any traction to the web and is therefore useless for tension regulation purposes. A calculation of this ratio appears in Table 1 and Table 2 as well as a calculation of the air float height, h_0 , of the web entering the vacuum pull roller as calculated using (2).

Graphs of the tension ratios (at slip) as a function of web speed are shown in figures 4 through 7. Dotted lines in these graphs indicate the tension ratio expected for a simply wrapped roller of equivalent friction with no applied vacuum or air entrainment effects. Figure 4 and Figure 5 are both at a vacuum level of 6.2 kPa with the only difference being whether T_{out} is greater or less than T_{in} . In Figure 6 are data obtained with a vacuum level of 12.5 kPa. In all three of these graphs, it is surprising to note that the most effective tension ratios are obtained with the lowest incoming tension, T_{in} , to the vacuum roller. The best explanation of this effect is that, with lower incoming web tension, the vacuum is

better able to pull the web into the vacuum grooves and therefore produce more effective traction on the roller.

In Figure 7 no vacuum was applied to the roller and it can be observed that all of the data converge to a value slightly greater than one at higher web speeds, with the incoming web tension having no effect on the ultimate high speed tension ratio. A solid line on Figure 7 is the prediction² for $T_{in} = 214$ N (4 pli) and the dot-dash line is for $T_{in} = 27$ N (0.5 pli) using equations (1), (2) and (4). The case where $T_{out} < T_{in}$ resulted in some anomalously large tension ratios at low speed given the initial friction value μ_0 . One explanation for these anomalous data is the web mechanically locking into the grooves and thus gaining additional traction at high web tension.

Since air entrainment seemed to play a major vacuum roller traction, a graph of all of the tension ratio data as a function of the entering air layer height, h_0 , is shown in Figure 8. All of the data series, except the last three (open markers), were for the case T_{out} greater than T_{in} . A solid curve is plotted which is representative of the traction available with no vacuum but not including the anomalous values mentioned above. With no vacuum, the available traction is nearly nonexistent for large entrained air layers. In all cases, the combination of low incoming web tension and high vacuum level provided the best traction regardless of the amount of entrained air. In fact, the very highest incoming web tensions of 107 N (2 pli) for $T_{out} > T_{in}$ and 214 N (4 pli) for $T_{out} < T_{in}$ performed little better than the no vacuum case. Because of the importance of the web-groove interaction, an attempt was made to image the web on the vacuum roller surface under test conditions.

WEB IMAGES ON THE VACUUM ROLLER

A high-speed camera system was set up to image the web on the vacuum roller surface at the location shown in Figure 2. While the clear PET was difficult to image, it was fairly easy to spot pockets of trapped air under the web. Figure 9 shows the web on the vacuum roller surface at low speed and 6.2 kPa of vacuum. The sharpness of the image and the very small air pockets indicate that the web is firmly pulled down to the roller surface. In Figure 10 the web is shown at 244 m/min and the same 6.2 kPa vacuum level. Again, the web image looks sharp in the vicinity of the vacuum grooves and a small region nearby indicating good contact to the roller surface. However, large pockets of trapped air are visible between the vacuum grooves. Figure 11 shows the web at the same web speed but no applied vacuum. Lack of image sharpness and large trapped air bubbles indicate that only small regions of the web are making contact with the roller. Even though there is no vacuum, the holes and grooves do permit some venting of entrained air, which can be observed on one edge of the grooves.

² It turns out the adjustment to the air layer, h_0 , given in (3) is nearly 25 μm and completely overwhelms the air layer values given in tables 1 and 2. For this reason, no adjustment was made to h_0 . Also, rather high values for the residual coefficient of friction, $\mu_f = 0.12$ and surface roughness $R_q = 3.4$ μm were also required to fit the measured data. This R_q is much higher than $R_a = 0.45$ μm measured on the roller surface. All in all, this simple traction calculation method did not predict the measured traction on a grooved roller very well for the case with no applied vacuum.

CONCLUSIONS

Traction on hole and groove style vacuum rollers is highly sensitive to the air layer entrained by smooth PET web. Photos of the web on these rollers show that only a portion of the web is in contact with the roller surface and thus contributing to the traction. In all cases webs with lower input tension were able to develop a greater relative tension change than those with higher input tension. While they could sustain large tension changes, webs with very high input tension performed similarly independent of vacuum level or even without applied vacuum. Much better traction was observed for output tension lower than the input tension, that is the vacuum roller was pulling rather than braking. For all input tension cases, the ratio between input and output tension appeared to be converging to a value of between 2:1 and 4:1 at the highest web speeds tested. This tension ratio is much lower than the > 10:1 ratios observed at low web speed but retains most of the traction that would be expected from a simply wrapped roller with no applied vacuum.

Roller traction models developed for idler rollers did a poor job of modeling the traction on the hole and groove vacuum roller with no applied vacuum. The complex nature of the web contact observed in the photos, indicates the need for sophisticated numerical models which can better represent the web conforming to the vacuum grooves. Comparison of these models with measured data should be carried out as well as the study of other vacuum roller designs.

ACKNOWLEDGMENTS

The author would like to thank Dan Carlson for his assistance in configuring the web line for these experiments, Ron Swanson for experimental advice and assistance in collecting data, and John Strand for setting up the camera system used to obtain images of the web on the vacuum roller. Finally, I would like to thank my management at 3M for their support of this research.

REFERENCES

1. Knox, K. L., and Sweeney, T. L., "Fluid Effects Associated with Web Handling," Industrial Engineering Chemical Process Design Development, Vol. 10, 1971, pp 201-205.
2. Hashimoto, H., "Improvement of Web Spacing Characteristics by Two Types of Guide Rollers," Proceedings of the Fifth International Conference on Web Handling, Oklahoma State University, Stillwater, Oklahoma, June 6-9, 1999, pp 561-581.
3. Zahlan, N., Jones, D. P., "Modeling Web Traction on Rollers," Proceedings of the Third International Conference on Web Handling, Oklahoma State University, Stillwater, Oklahoma, June 13-21 1995, pp 156-171
4. Ducotey, K. S., "Traction Between Webs and Rollers in Web Handling Applications," PhD Dissertation, Oklahoma State University.
5. Good, J. K., "Shear in Multispan Web Systems," Proceedings of the Fourth International Conference on Web Handling, Oklahoma State University, Stillwater, Oklahoma, June 1-4, 1997, pp 264-286
6. LSV-065, Polytec GmbH, Waldbronn, Germany.

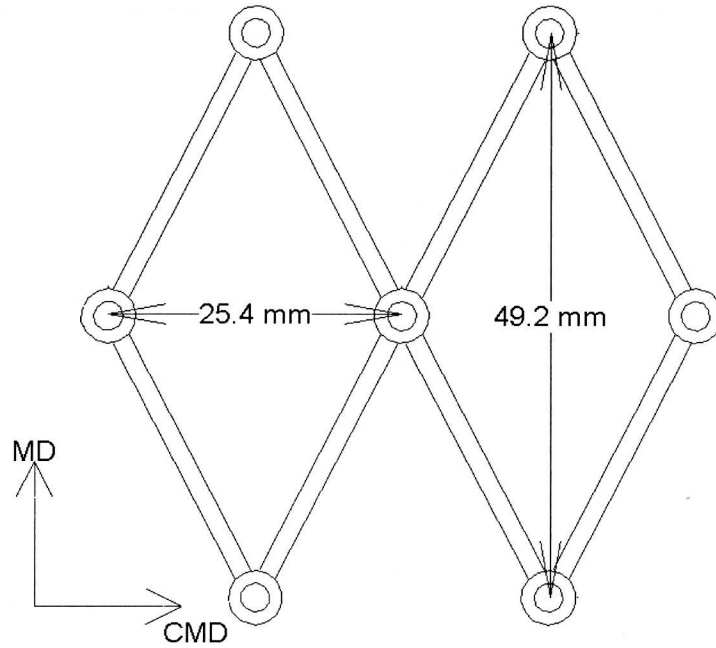


Figure 1 Vacuum roller hole and groove pattern. Grooves are square in section with a width of 1.25 mm and depth of 0.25 mm.

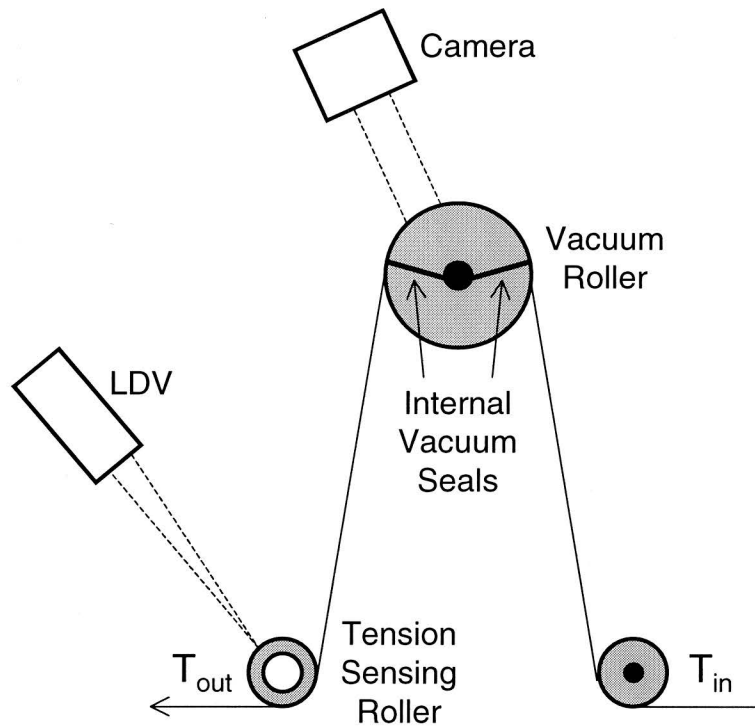


Figure 2 Experimental setup used for traction testing of vacuum roller.

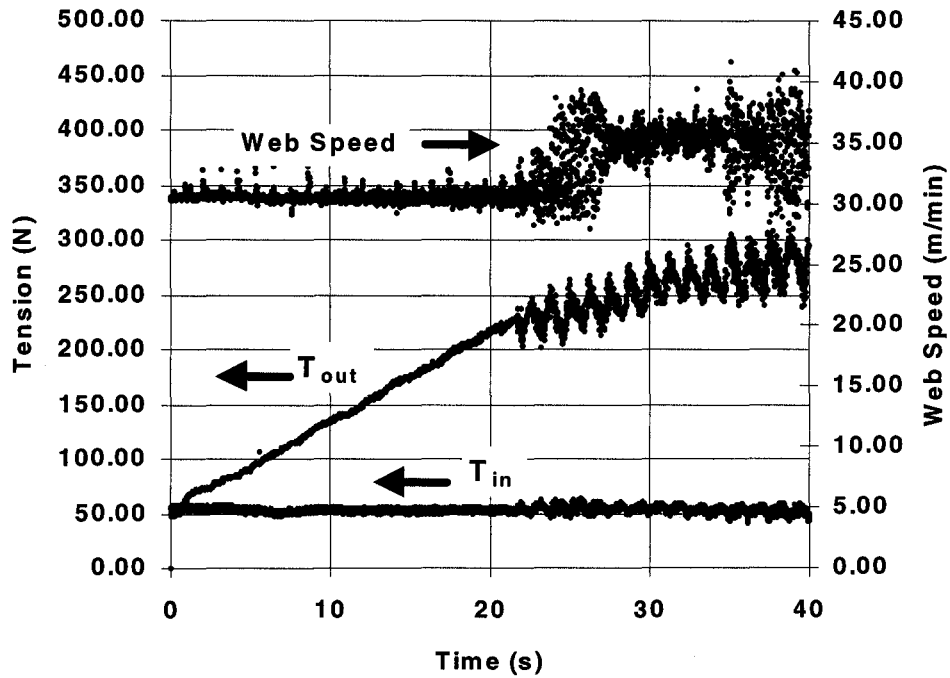


Figure 3 Graph of web speed and tension during a traction test.

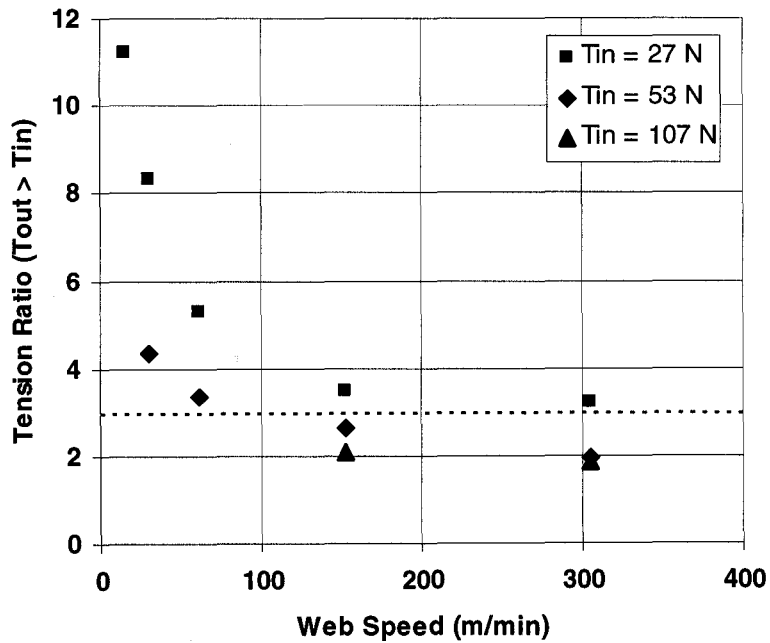


Figure 4 Tension ratio at slip for $T_{out} > T_{in}$ and a vacuum level of 6.2 kPa. Dotted line represents traction expected with no vacuum or air entrainment.

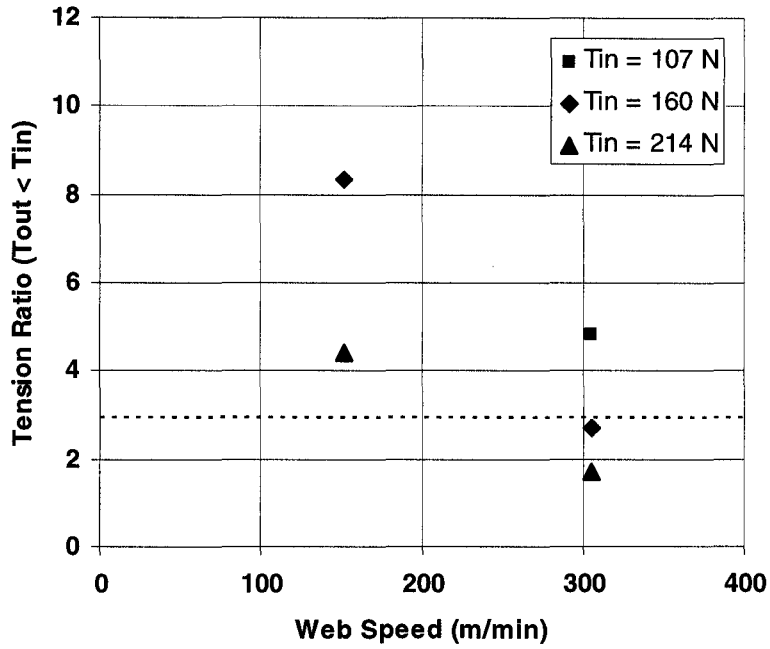


Figure 5 Tension ratio at slip for $T_{out} < T_{in}$ and a vacuum level of 6.2 kPa. Dotted line represents traction expected with no vacuum or air entrainment.

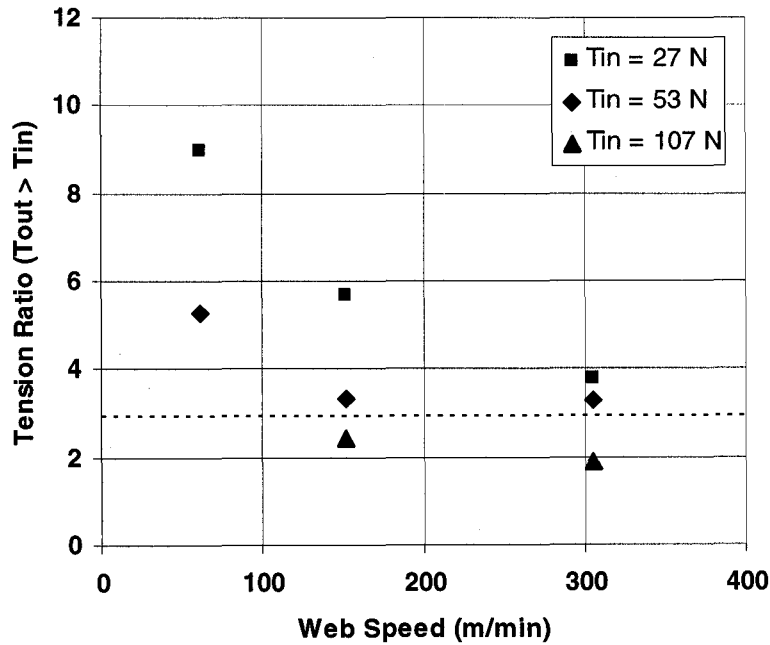


Figure 6 Tension ratio at slip for $T_{out} > T_{in}$ and a vacuum level of 12.5 kPa. Dotted line represents traction expected with no vacuum or air entrainment.

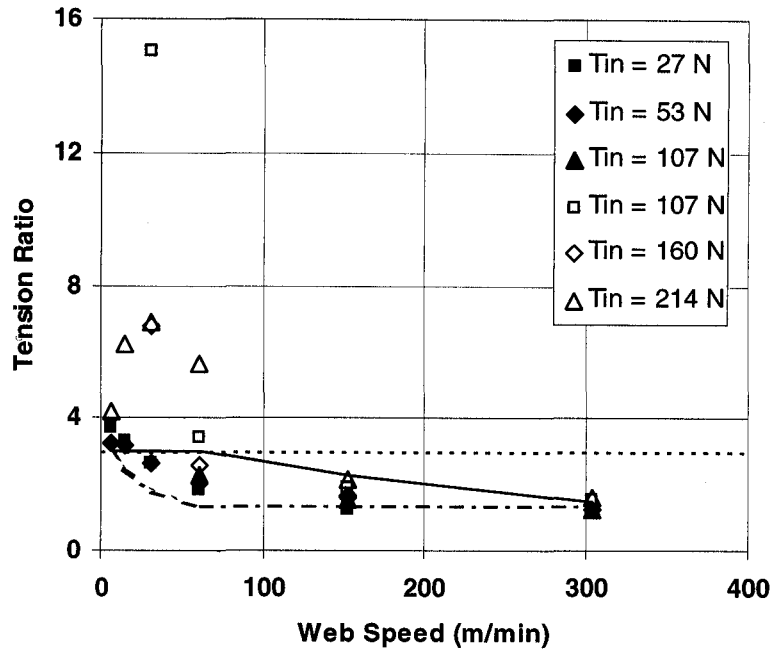


Figure 7 Tension ratio for $T_{out} > T_{in}$ (filled) and $T_{out} < T_{in}$ (open) with no vacuum applied. Dotted line represents traction expected with no vacuum or air entrainment. Solid and dot-dash lines are no vacuum, air lubricated, tractions predicted for $T_{in} = 214$ N (4 pli) and $T_{in} = 27$ N (0.5 pli) respectively.

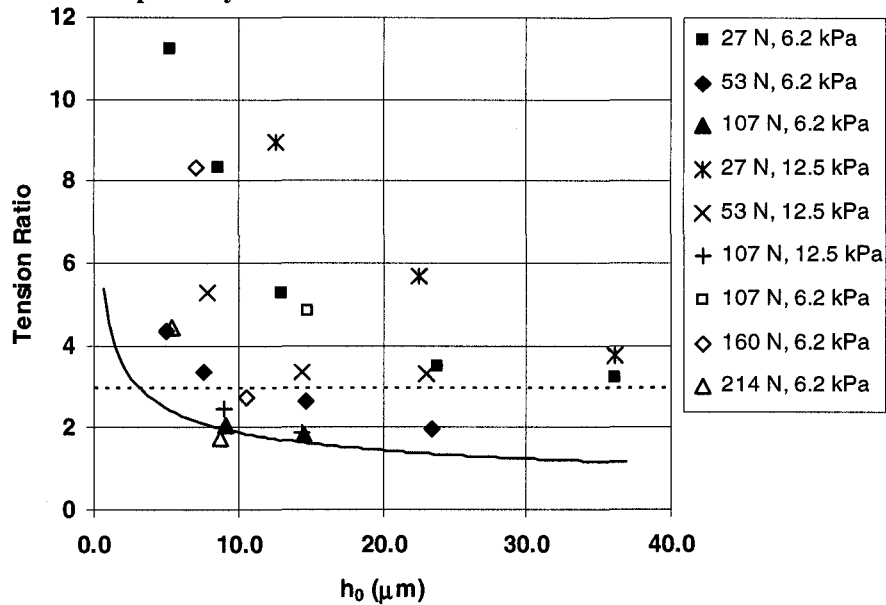


Figure 8 Tension ratio as a function of entrained air layer height h_0 . Solid line represents the no vacuum tension ratios of Figure 7. Dotted line is traction expected with no vacuum or air entrainment.

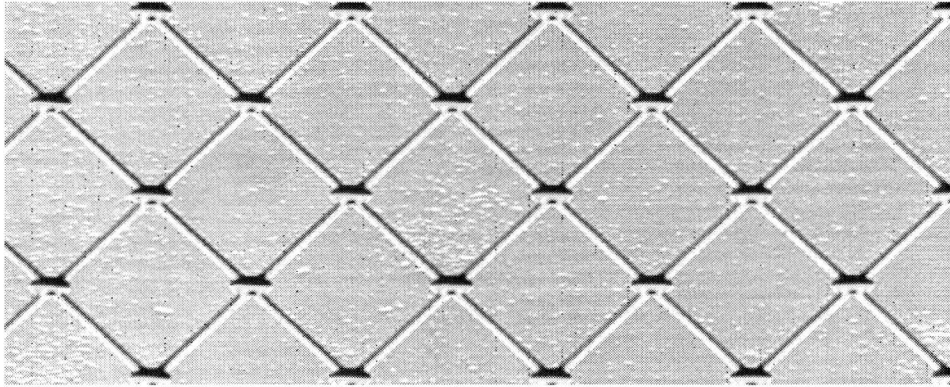


Figure 9 Image of web on surface of vacuum roller with vacuum level at 6.2 kPa and web speed of 15 m/min.

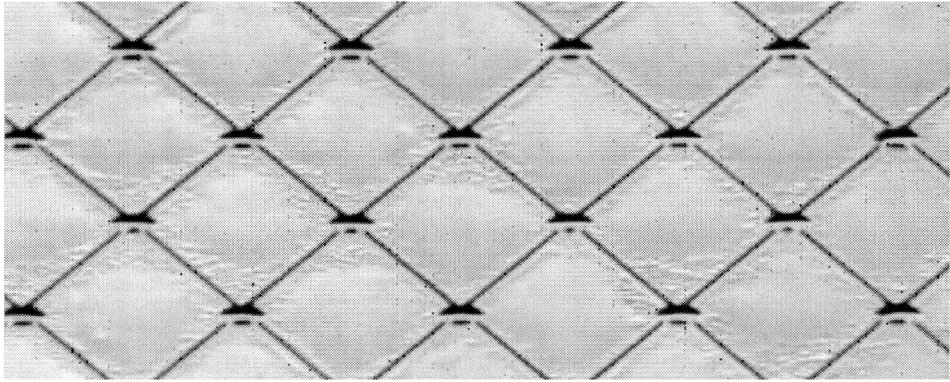


Figure 10 Image of web on surface of vacuum roller with vacuum level at 6.2 kPa and web speed of 244 m/min.

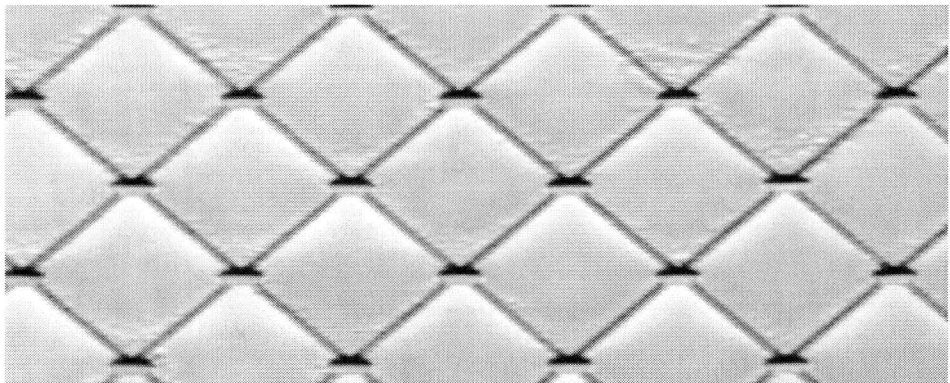


Figure 11 Image of web on surface of vacuum roller with no vacuum and web speed of 244 m/min. Blurring in the image is from the web lifting off of the roller and out of the vacuum grooves.

Web Speed (m/min)	Vacuum (kPa)	T _{in} (N)	T _{out} (N)	T _{out} /T _{in}	h ₀ (μm)
6	6.2	50	* 314	> 6.3	1.8
15	6.2	54	* 316	> 5.8	3.1
30	6.2	53	229	4.3	5.0
61	6.2	56	188	3.3	7.5
152	6.2	52	137	2.6	14.7
305	6.2	52	101	2.0	23.4
6	6.2	24	* 315	> 12.9	2.9
15	6.2	24	274	11.2	5.3
30	6.2	24	196	8.3	8.6
61	6.2	25	134	5.3	12.9
152	6.2	25	88	3.5	23.8
305	6.2	27	87	3.2	36.1
6	6.2	111	* 313	> 2.8	1.0
15	6.2	106	* 313	> 3.0	2.0
30	6.2	105	* 313	> 3.0	3.1
61	6.2	106	* 315	> 3.0	4.9
152	6.2	105	218	2.1	9.2
305	6.2	104	192	1.8	14.6
6	12.5	54	* 313	> 5.8	1.7
15	12.5	54	* 311	> 5.7	3.1
30	12.5	54	* 311	> 5.7	4.9
61	12.5	54	285	5.3	7.8
152	12.5	53	179	3.4	14.4
305	12.5	53	175	3.3	23.0
6	12.5	19	* 312	> 16.0	3.3
15	12.5	26	* 314	> 12.0	5.0
30	12.5	27	* 312	> 11.7	7.9
61	12.5	26	235	9.0	12.6
152	12.5	28	156	5.7	22.5
305	12.5	27	102	3.8	36.1
6	12.5	112	* 314	> 2.8	1.0
15	12.5	108	* 313	> 2.9	1.9
30	12.5	107	* 312	> 2.9	3.1
61	12.5	106	* 312	> 2.9	4.9
152	12.5	108	264	2.5	9.0
305	12.5	107	200	1.9	14.4
6	0.0	54	177	3.3	1.7
15	0.0	55	174	3.2	3.0
30	0.0	54	141	2.6	4.9
61	0.0	55	112	2.0	7.7
152	0.0	54	86	1.6	14.3
305	0.0	52	66	1.3	23.4
6	0.0	24	87	3.7	2.9
15	0.0	25	83	3.3	5.1
30	0.0	26	69	2.6	8.0
61	0.0	26	49	1.9	12.6
152	0.0	28	36	1.3	22.3
305	0.0	26	30	1.1	37.0
6	0.0	113	* 298	> 2.6	1.0
15	0.0	108	* 298	> 2.8	1.9
30	0.0	105	* 291	> 2.8	3.1
61	0.0	107	241	2.3	4.9
152	0.0	104	159	1.5	9.2
305	0.0	106	132	1.2	14.4

Table 1 Vacuum roller traction data for T_{out} > T_{in}

* Indicates a test where no web slippage could be developed across the roller.

Web Speed (m/min)	Vacuum (kPa)	T _{in} (N)	T _{out} (N)	T _{in} /T _{out}	h ₀ (μm)
6	6.2	213	* 5	> 38.9	0.7
15	6.2	213	* 5	> 38.9	1.2
30	6.2	217	* 4	> 52.6	1.9
61	6.2	215	* 5	> 47.0	3.1
152	6.2	229	52	4.4	5.4
305	6.2	223	129	1.7	8.8
6	6.2	105	* 2	> 44.7	1.1
15	6.2	104	* 1	> 70.9	2.0
30	6.2	108	* 3	> 33.3	3.1
61	6.2	102	* 2	> 43.2	5.1
152	6.2	103	* 3	> 36.6	9.3
305	6.2	102	21	4.8	14.8
6	6.2	61	* 2	> 26.0	1.5
15	6.2	58	* 2	> 30.4	2.9
30	6.2	53	* 3	> 16.4	4.9
61	6.2	55	* 2	> 23.2	7.7
152	6.2	52	* 3	> 18.7	14.6
305	6.2	55	* 8	> 6.7	22.5
6	6.2	162	* 2	> 68.7	0.8
15	6.2	163	* 2	> 69.0	1.5
30	6.2	158	* 4	> 38.3	2.4
61	6.2	159	* 1	> 108.2	3.8
152	6.2	153	18	8.3	7.1
305	6.2	169	62	2.7	10.6
6	12.5	104	* 11	> 9.7	1.1
15	12.5	107	* 5	> 19.6	1.9
30	12.5	104	* 6	> 17.5	3.2
61	12.5	109	* 5	> 19.9	4.8
152	12.5	101	* 5	> 18.4	9.4
305	12.5	102	* 8	> 13.2	14.8
6	0.0	216	52	4.2	0.7
15	0.0	209	33	6.3	1.2
30	0.0	213	31	6.9	2.0
61	0.0	212	37	5.6	3.1
152	0.0	206	97	2.1	5.8
305	0.0	193	118	1.6	9.7
6	0.0	101	* 7	> 13.9	1.1
15	0.0	104	* 7	> 14.3	2.0
30	0.0	102	7	15.0	3.2
61	0.0	100	29	3.4	5.1
152	0.0	100	51	1.9	9.5
305	0.0	96	62	1.6	15.4
6	0.0	50	* 3	> 17.9	1.8
15	0.0	52	* 3	> 18.6	3.2
30	0.0	55	8	6.8	4.8
61	0.0	55	21	2.6	7.7
152	0.0	49	29	1.7	15.2

Table 2 Vacuum roller traction data for T_{out} < T_{in}

* Indicates a test where no web slippage could be developed across the roller.

Name & Affiliation	Question
K. Good – OSU	The effect of the shading was good in your pictures. Would it not be possible to put the light source laterally so if the tension was what was pulling that web down into the grooves so you'd see shadows laterally? Could we judge from lateral shadows what the depth is that the plastic is being pulled down into the grooves?
Name & Affiliation	Answer
J. Dobbs – 3M	I showed the location of camera, but not the light source. The lighting you are asking about was used.
Name & Affiliation	Question
B. Walton – Eastman Kodak Company	How big were the holes in the vacuum drum?
Name & Affiliation	Answer
J. N. Dobbs – 3M	About 3/16 of an inch, but they had a rather large chamfer.
Name & Affiliation	Question
J. J. Shelton – OSU	There are some really long vacuum rollers in existence. I wonder whether you have any vacuum at the center or not. I know that this wasn't any problem for your length of roller for length of your test roller and the speed. With the velocity of sound at 1100 ft per second there are bound to be pressure waves shuttling back and forth.
Name & Affiliation	Answer
J. N. Dobbs – 3M	Our test roller was only 20 inches wide. I suppose you would have to take sound waves into consideration for very large vacuum drive rollers.